Journal of Electrical Systems and Information Technology

RESEARCH Open Access

Transient stability enhancement of Beles to Bahir Dar transmission line using adaptive neuro-fuzzy-based unified power flow controller

Yechale Amogne Alemu[1*], Tefera Terefe Yetayew[2] and Molla Addisu Mossie[2]

*Correspondence:
yechaleamogne12@gmail.com

[1] Faculty of Electrical and Computer Engineering, Woldia Institute of Technology (WiT), Woldia University, P.O. Box 400, Woldia, Ethiopia
[2] Faculty of Electrical and Computer Engineering, Bahir Dar Institute of Technology (BiT), Bahir Dar University, P.O. Box 26, Bahir Dar, Ethiopia

Abstract

A power system is a complex, nonlinear, and dynamic system, with operating parameters that change over time. Because of the complexity of big load lines and faults, high-voltage transmission power systems are usually vulnerable to transient instability concerns, resulting in power losses and increased voltage variation. This issue has the potential to cause catastrophic events such as cascade failure or widespread blackouts. This problem affects Ethiopia's high-voltage transmission power grid in the northwest area. Because of the increased demand for electrical energy, transmission lines' maximum carrying capacity should be enhanced to maintain a secure and uninterrupted power supply to consumers. To address the problem, ANFIS-based UPFC is used for high-voltage transmission lines. This device was chosen as the ideal alternative due to its capacity to rapidly correct reactive power on high-voltage transmission networks. The PSO algorithm was used to determine the best location for the UPFC. The ANFIS controller receives voltage error and rate of change of voltage error as inputs. Seventy percentage of the retrieved data are used for ANFIS training and 30% for ANFIS testing. To show the performance of the proposed controller, three-phase ground faults are used from a severity perspective. When a three-phase ground fault occurs at the midpoint of the Beles to Bahir Dar transmission line, for instance, the settling time of rotor angle deviation, rotor speed, rotor speed deviation, and output active power of synchronous generators using ANFIS-based UPFC is reduced by 70.58%, 37.75%, 37.75%, and 43.75%, respectively, compared to a system without UPFC. At peak load, PI-based UPFC and ANFIS-based UPFC reduce active power loss by 51.25% and 71.50%, respectively, compared to a system without UPFC on the Beles to Bahir Dar transmission line. In terms of percentage overshoot and settling time, ANFIS-based UPFC outperforms PI-based UPFC for transient stability enhancement.

Keywords: FACTs, UPFC, PI controller, ANFIS, Power system, PSO

Introduction

Power systems are complex nonlinear and dynamic systems, with operating parameters that change over time. Because of the dynamic nature of the power system, frequent disturbances have the potential to drive it into an unstable condition. The power system's dependability and power quality index will both suffer as a result of the constant

disturbances [1–3]. The capacity of the power system to sustain synchronization after a rapid and large disturbance is referred to as transient stability. These changes might occur as a result of rapid load application, generation loss, loss of a significant load, or system failure. Multiple synchronous generators are attached to the same bus in power plants, sharing similar frequency and phase sequences. As a result, in order to ensure stability during the whole generation and transmission process, the bus must be continuously synchronized with the generators [4–6].

The unified power flow controller (UPFC) is the most versatile of the FACTS devices available for increasing system stability. The UPFC, which is made up of two AC-to-DC converters, can both deliver and absorb actual and reactive power. One of the converters is linked in series with the transmission line using a series transformer, while the other is connected in parallel with the line through a shunt transformer. The DC side of both converters is interconnected by a shared capacitor, which supplies the necessary DC voltage for their operation [7, 8]. Various advanced control approaches are used and simulated to regulate the UPFC's input parameters. Fuzzy logic and neural networks are used to offer robust control and transient stability over a wide range of power system operating situations [9–11]. FACT devices contribute to the stability of a large power system with numerous buses by providing dynamic control over voltage, power flow, and system parameters. Their ability to quickly respond to changes in the network helps in maintaining stability under varying operating conditions and disturbances [12–14]. The rest of this paper is organized with the proposed methodology in Section II; simulation results and discussion are presented in Section IV; and conclusions are presented in Section V.

Methodology

The use of FACTS devices, which have rapid and smooth switching characteristics made possible by power electronics technology, is one of the many approaches available to improve transient stability. Transient stability refers to the power system's capacity to maintain synchronization in the face of abrupt and significant disturbances. Such disruptions can arise from rapid load changes, generation loss, large-scale load shedding, or system faults. The adaptive neuro-fuzzy-based unified power flow controller (UPFC) is a device that can both inject and absorb real and reactive power. It is made up of two AC-to-DC converters [15, 16]. The schematic representation of a basic UPFC is shown in Fig. 1.

VSC1 is connected to the transmission line in parallel through a shunt transformer, whereas VSC2 is connected in series using a series transformer. The two VSCs are interconnected through DC terminals, creating a pathway for active power exchange between the converters. The VSC performs the principal function of the UPFC by introducing a voltage with a controlled magnitude and phase angle into the line through an injection transformer. The voltage injected serves as a synchronous alternating current (AC) power source [4]. The voltage source causes current to flow down the transmission line, resulting in the interchange of reactive and active power with the alternating current system. The reactive power exchanged at the DC terminal is generated internally by the converter. The real power is transformed to DC power at the AC terminal and then

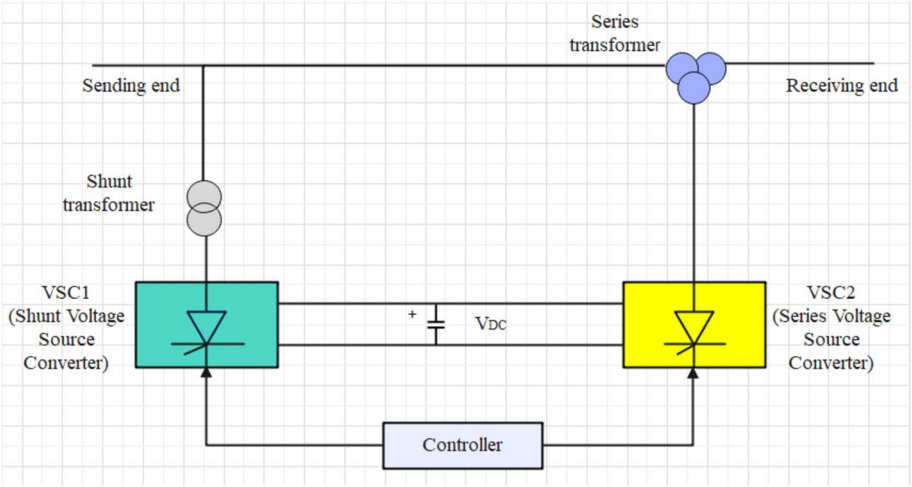

Fig. 1 Basic UPFC schematic diagram

appears as a demand for real power at the DC link [17]. Figure 2 is a single-line schematic of Ethiopia's high-voltage power grid in the northwest region.

Mathematical modeling unified power flow controller

Mathematical modeling of shunt converter controller

Figure 3 depicts a unified power flow controller's conventional circuit architecture. The diagram of the D-Q frame shunt converter control of the UPFC is shown in Fig. 4, while Fig. 5 presents the Simulink model of the shunt converter controller.

The shunt converter in the a-b-c reference axis system gives rise to a differential equation obtained UPFC shunt circuit. By applying Park's transformation, the three-phase system can be transformed into the d-q axis. Reference of the output of the shunt converter, V_{shd}^* and V_{shq}^* is as follows [18]:

$$\begin{bmatrix} V_{shd}^* \\ V_{shq}^* \end{bmatrix} = \begin{bmatrix} k_{psh} + \frac{k_{ish}}{s} & 0 \\ 0 & k_{psh} + \frac{k_{ish}}{s} \end{bmatrix} * \begin{bmatrix} i_{shd}^* - i_{shd} \\ i_{shq}^* - i_{shq} \end{bmatrix} + \begin{bmatrix} V_{1d} + \omega i_{shq} \\ -\omega i_{shd} \end{bmatrix} \quad (1)$$

Mathematical modeling of series converter controller

The series converter in the a-b-c reference axis system gives rise to a differential equation obtained UPFC circuit. By applying Park's transformation, the three-phase system can be transformed into the d-q axis. Reference of the output of the series converter V_{sed}^* and V_{seq}^* is as follows [18]:

$$\begin{bmatrix} V_{sed}^* \\ V_{seq}^* \end{bmatrix} = \begin{bmatrix} k_{pse} + \frac{k_{ise}}{s} & 0 \\ 0 & k_{pse} + \frac{k_{ise}}{s} \end{bmatrix} * \begin{bmatrix} i_{sed}^* - i_{sed} \\ i_{seq}^* - i_{seq} \end{bmatrix} + \begin{bmatrix} V_{rd} - V_{1d} - \omega i_{seq} \\ -V_{1q} + \omega i_{sed} \end{bmatrix} \quad (2)$$

The series converter control diagram is shown in Fig. 6.

Taking the mathematical modeling of series converter controller, MATLAB/SIMULINK model was designed. The overall Simulink model of series controller is as depicted in Fig. 7.

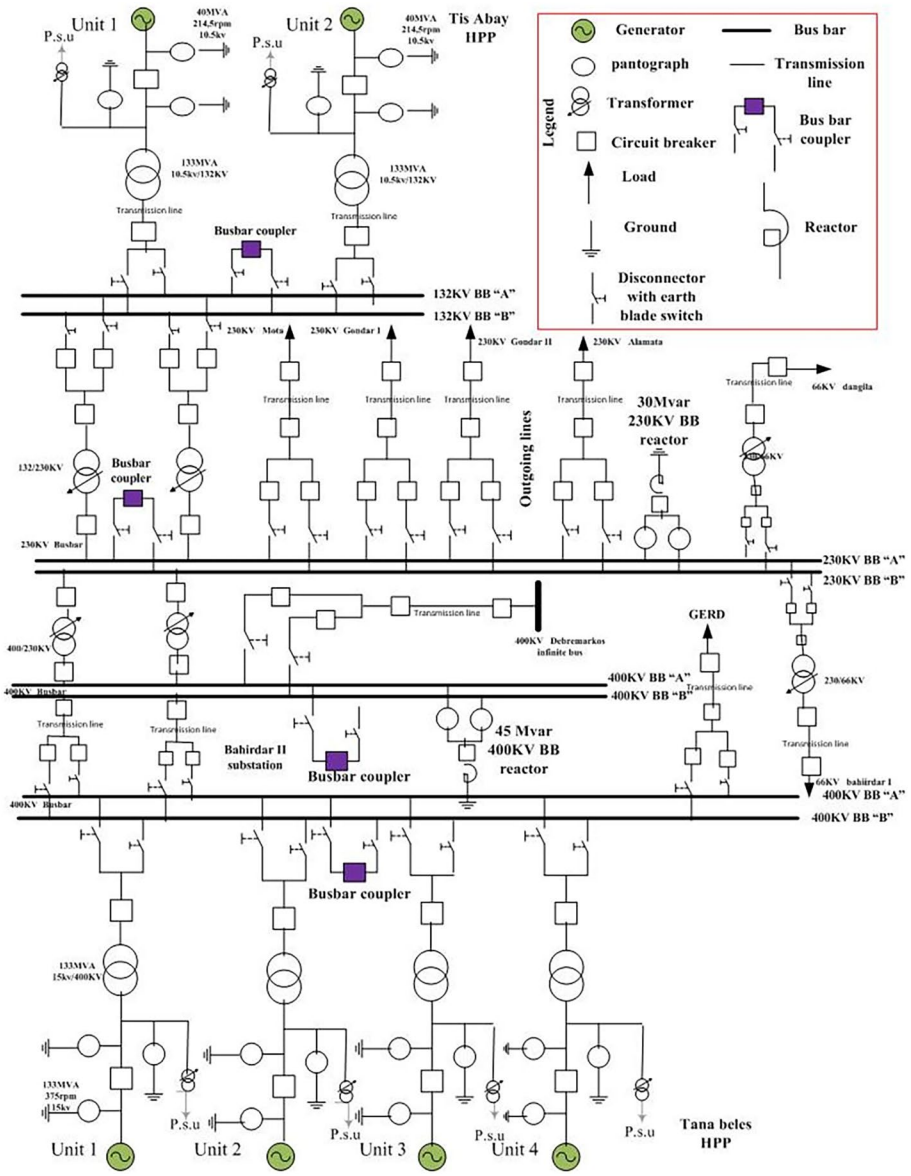

Fig. 2 Single-line diagram of the northwest region network

Design of ANFIS-based UPFC and its optimal location

Optimal location of UPFC using PSO algorithm

The objective function is to minimize transmission loss by adjusting control variables within their specified limits. As a result, the system constraints need to be defined as a combination of equality and inequality constraints.

Objective function

Objective function = Min F(P_{loss}).

The real power loss of the system equals the sum of the real power loss on each branch, and it can be described as follows [5]:

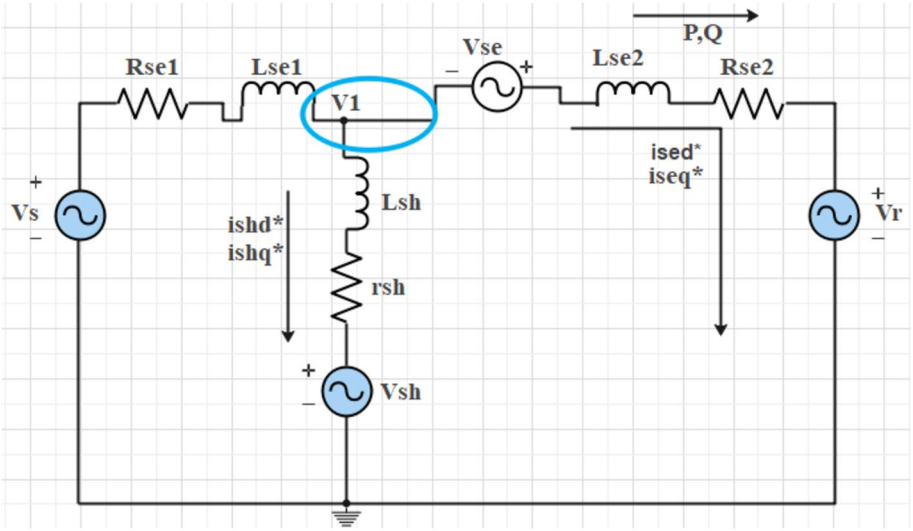

Fig. 3 Single-phase circuit representation of a power flow in UPFC

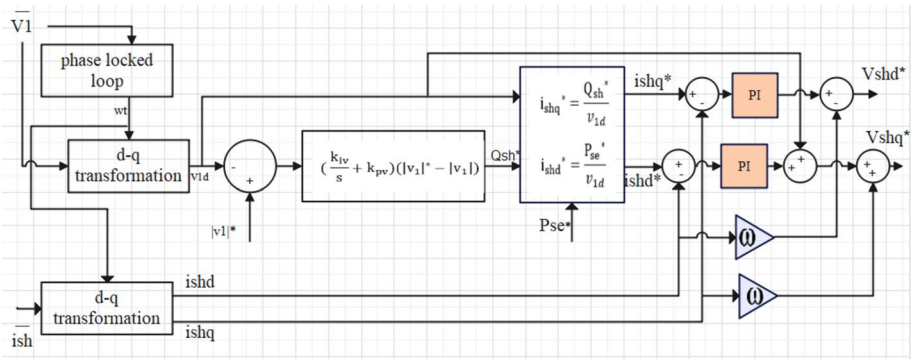

Fig. 4 D-Q frame shunt converter control of UPFC

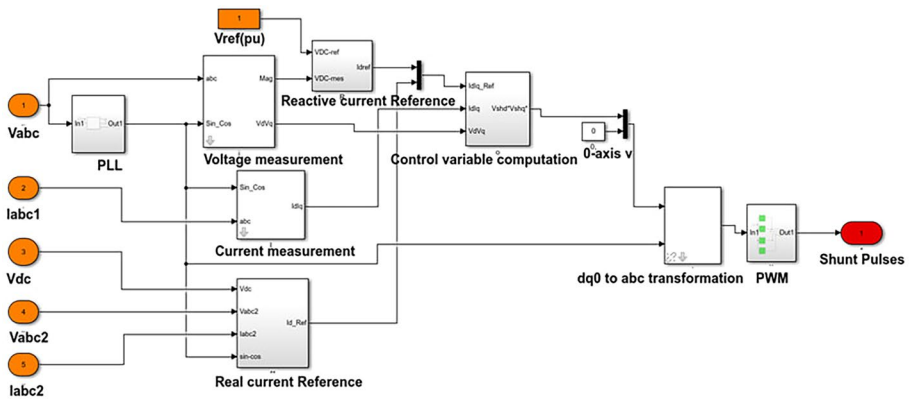

Fig. 5 SIMULINK model of shunt converter controller

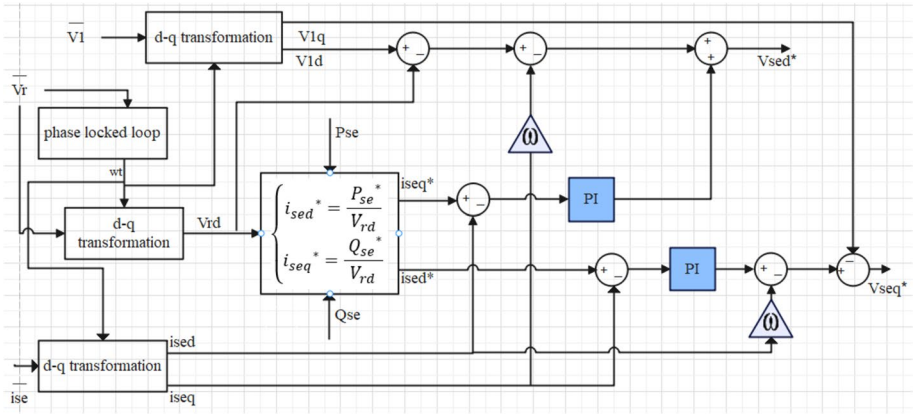

Fig. 6 D-Q frame of series converter control of UPFC

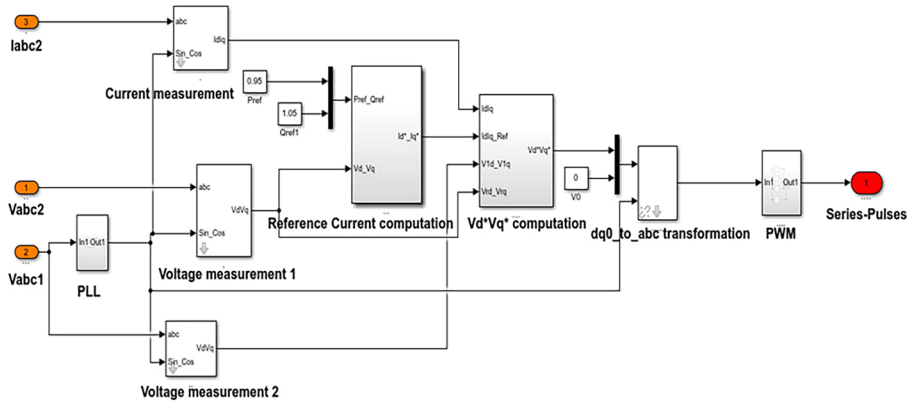

Fig. 7 SIMULINK models of series converter controller

$$F : P_{loss} = \sum_{i \in j}^{N} Gij \left(V_i^2 + V_j^2 - 2V_i V_j \cos\theta_{ij} \right) \tag{3}$$

where: N is the number of the branches, Gij is the conductance between bus i and bus j, V_i is the voltage magnitude of bus I, V_j is the voltage magnitude of bus j, and θ_{ij} s the difference angle between bus i and bus j.

Equality constraints

The power balance equations represent the equality constraints, which can be mathematically expressed by the following equations [5]:

$$P_{gi} - P_{di} - V_i \sum_{j=1}^{NP} V_j (Gij \cos\theta_{ij} + Bij \sin\theta_{ij}) = 0 \tag{4}$$

$$Q_{gi} - P_{di} - V_i \sum_{j=1}^{NQ} V_j (Gij \sin\theta_{ij} - Bij \cos\theta_{ij}) = 0 \tag{5}$$

where P_{gi} is the real power generation at bus i, P_{di} is the real power demand at bus i, Q_{gi} is the real power generation at bus i, and Q_{di} is the real power demand at bus i.

Inequality constraints

The inequality constraints taken is bus voltage magnitude [5].

$$V_i^{min} < V_i < V_i^{max} \tag{6}$$

The per unit bus voltage value should be within the prescribed limit (i.e., with ±5% in the range of $0.95 \leq vi \leq 1.05$).

The penalty function

The penalty function for bus voltages is shown in the equation below [19].

$$\Omega_v = \rho \sum_{i=1}^{N_B} \left\{ \max\left(0, |V_i| - |V_i^{max}|\right) \right\}^2 + \rho \sum_{i=1}^{N_B} \left\{ \max(0, |V_i^{min}| - |V_i|) \right\}^2 \tag{7}$$

where; Ω_v is the penalty function for bus voltages. ρ is the penalty factor. V_i^{max} is upper limit magnitude of voltage at bus i. V_i^{min} is lower limit magnitude of voltage at bus i.

The flowchart of the modified PSO for UPFC placement is shown in Fig. 8.

If the bus voltage value is greater than or less than the prescribed limit, it will be penalized by changing value of penalty factor-based equation given in Eq. (7). This adjustment is intended to guide the PSO algorithm in placing the unified power flow controller (UPFC) device on the appropriate bus. The altered penalty factor influences the optimization process, helping to ensure that the UPFC is positioned in a

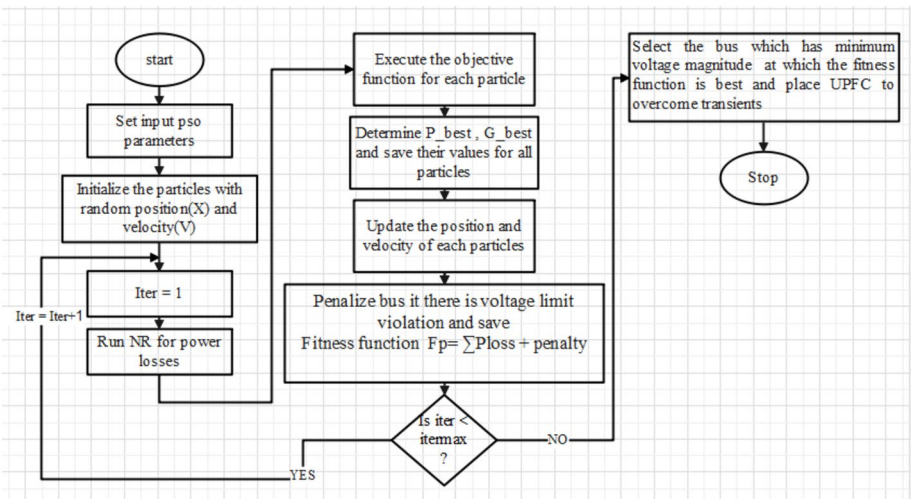

Fig. 8 Flowchart of the modified PSO for UPFC placement

Table 1 PSO parameters used for UPFC placement

PSO parameter	Value
Cognitive factor-min (C1)	1.5
Cognitive factor-max (C1)	2.5
Social factor-min (C2)	1.5
Social factor-max (C2)	2.5
Inertia weight-min (Wmin)	0.4
Inertia weight max (Wmax)	0.9
Maximum No. of iteration	50
Population size	100

Table 2 Bus voltage magnitude using modified PSO at three different loading scenarios

Bus No.	Bus location	Voltage magnitude (p.u) at peak load	Voltage magnitude (p.u) at average load	Voltage magnitude (p.u) at light load
1	Tana Beles	1.0200	1.0200	1.0200
2	Tis Abay II	1.0100	1.0100	1.0100
3	Bahir Dar 400 kV	0.9365	0.9421	0.9539
4	Bahir Dar 230 kV	0.9365	0.9489	0.9549
5	Bahir Dar 132 kV	0.9532	0.9549	0.9563
6	D/markos 400 kV	0.9532	0.9569	0.9683
7	D/markos 230 kV	0.9432	0.9559	0.9682
8	Motta 230 kV	0.9532	0.9579	0.9683
9	Alamata 230 kV	0.9432	0.9529	0.9533
10	Gonder I 230 kV	0.9570	0.9608	0.9631
11	Gonder II 230 kV	0.9548	0.9612	0.9634

way that aligns with the desired criteria or constraints related to the bus voltage values. Essentially, the modification aims to improve the efficiency and effectiveness of the PSO algorithm in determining the optimal placement of the UPFC device on the power system buses. The PSO parameters used for the UPFC placement are presented in Table 1, while the bus voltage magnitude using the modified PSO at three different loading scenarios is presented in Table 2.

Based on the proposed algorithm, the Bahir Dar 400 kV bus bar is the selected bus to place UPFC, as its magnitude is 0.9365, 0.9421, and 0.9539 (i.e., a low voltage magnitude bus with the lowest value, which is ranked as the weakest bus) for peak load, average load, and light load, respectively.

Design of ANFIS-based unified power flow controller

A neuro-fuzzy system refers to a fuzzy system that acquires its parameters, including fuzzy sets and fuzzy rules, through the utilization of a learning algorithm derived from or inspired by neural network theory. This concept was introduced by Jang in 1993 and involves the automatic generation of a fuzzy rule base and membership functions by processing data samples [20]. A typical illustration of the neuro-fuzzy inference system (ANFIS) architecture is shown in Fig. 9.

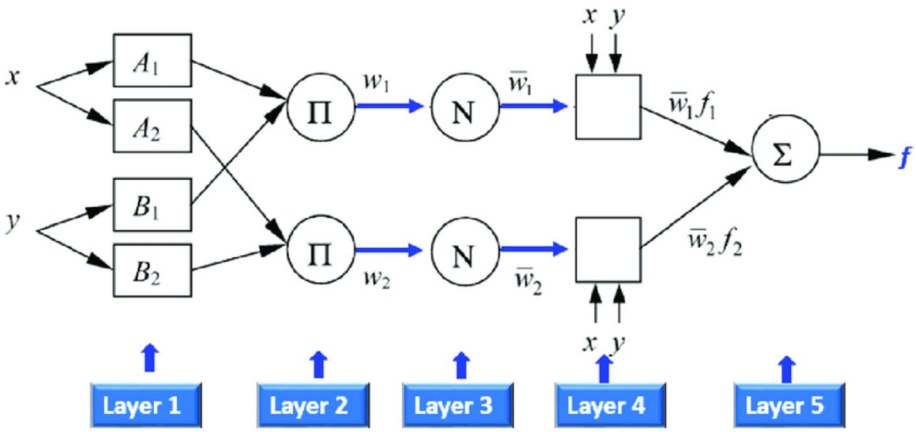

Fig. 9 Neuro-fuzzy inference system (ANFIS) architecture

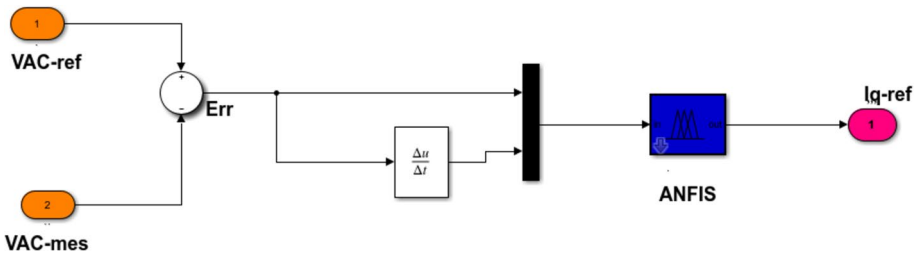

Fig. 10 ANFIS-based iq-reference computation

The ANFIS controller receives an input consisting of the error (e) and the derivative of the error (de/dt) and produces a single output (I-qref). The selection of the quadrature component current based on the real error is motivated by the fact that when the quadrature reference current generated by the unified power flow controller (UPFC) is perpendicular to the line current, it directly affects the reactance of the line, thereby regulating the flow of real power [21]. When the quadrature component of the reference current generated by the UPFC is set based on the real error (the error in real power flow), it implies that the control system is designed to respond to deviations in real power by adjusting the reactive power injection. The idea is that when the quadrature reference current is perpendicular to the line current, it directly impacts the reactance of the line. In electrical systems, the real power (P) is given by the product of voltage (V), current (I), and the power factor (cosine of the phase angle difference between voltage and current). By adjusting the quadrature component of the current, the control system can influence the reactive power (Q) component, which is proportional to the sine of the phase angle. This adjustment in reactive power can, in turn, impact the overall power factor and, importantly, the reactance of the line. Controlling the reactance of the line allows for the regulation of real power flow. When the reactive power injection is adjusted such that, it is perpendicular to the line current, it can effectively influence the impedance of the line and, consequently, control the flow of real power. Figure 10 displays the computation of iq-reference using the adaptive neuro-fuzzy inference system (ANFIS), while Fig. 11 depicts the ANFIS-based computation of id-reference.

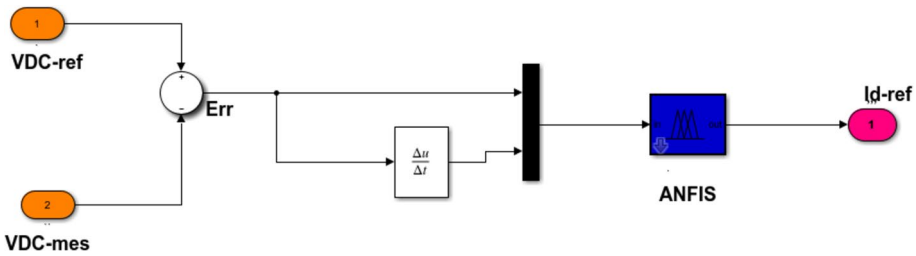

Fig. 11 ANFIS-based id-reference computation

Additionally, incorporating the error and its derivative as inputs to the controller enables more effective design of the rule base as it captures the physical behavior of the system during transient disturbances like faults.

Results and discussion

The simulation result of the model reveals the transient stability of an ANFIS-based UPFC connected in the northwest region to a high voltage, 256.54 km interconnected long transmission power system that covers Tana Beles to Debre Markos with its equivalent transmission line impedances, transformer parameters, and loads. This demonstrates the transient stability enhancement of the northwest region interconnected power system under different disturbance scenarios. PSO is used to identify the weakest bus of the test system for optimal placement of UPFC. Using this method, the Bahir Dar substation's 400 kV bus bar is the appropriate place for UPFC to work effectively.

The simulation is conducted using MATLAB/SIMULINK software, and different performance indices are recorded to compare and validate the designed controller. To validate the designed controller, ANFIS data are extracted for training and testing from the PI input and output of the voltage regulator. The input is error and error derivatives of the voltage regulator, while the output is direct and quadrature current output. The triangular membership function is chosen for the ANFIS set as it proves to be effective in mapping non-fuzzy input values to fuzzy linguistic terms in the context of transient stability enhancement. 300,000 rows of data have been extracted from the PI-based UPFC. To validate ANFIS, 30% of the extracted data are used for the ANFIS test, and the remaining 70% are for the ANFIS train. Finally, the effectiveness of ANFIS-based UPFC is tested by comparing its performance, such as its power transfer capacity, loss reduction, and voltage profile improvement. The system response is analyzed without UPFC, with PI-based UPFC, and with ANFIS-based UPFC. The PI parameters found by the autotuning technique are $Kp = 10$ and $Ki = 0.1$. In this section, the ability of the system to maintain synchronism at the generation level for a disturbance that occurred at the transmission line has been observed with different performance indices, such as settling time and maximum overshoot. The system model and UPFC site location is shown in Fig. 12. To test the proposed method in this paper, three-phase ground faults are applied from a severity perspective.

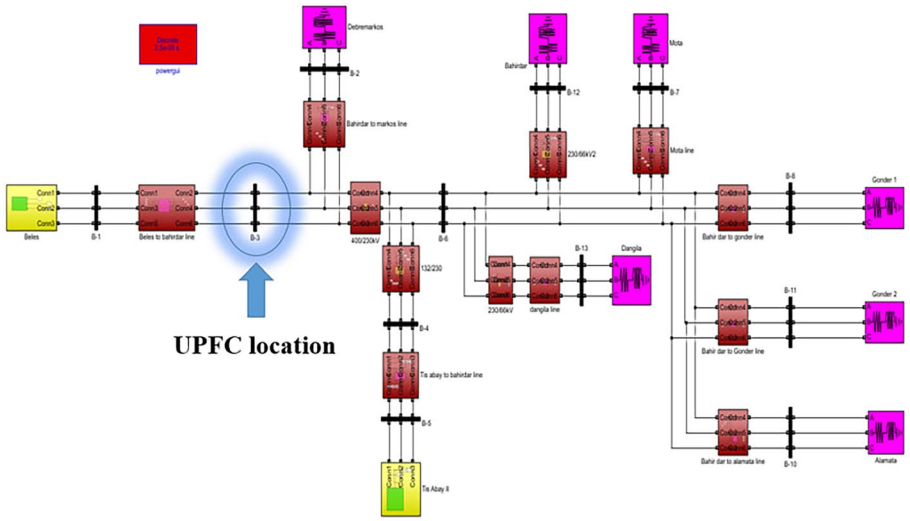

Fig. 12 System model and UPFC site location

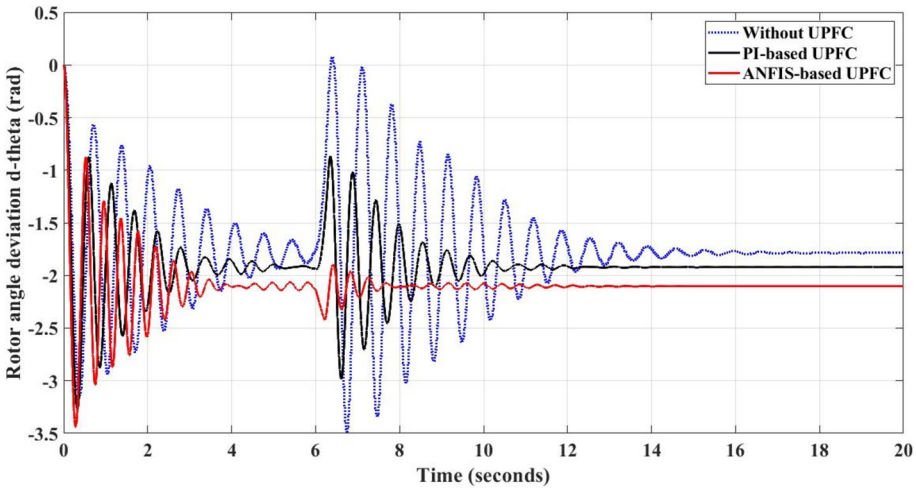

Fig. 13 Rotor angle deviation response of Beles Unit-3 for 3ph-G fault occurred at the midpoint of the Tana Beles to Bahir Dar line

System response when a 3ph-G fault occurred at the midpoint of the *Tana* Beles to Bahir Dar transmission line

Figures 13, 14, 15, and 16 display the responses of rotor angle deviation, rotor speed, output active power, and rotor speed deviation for generators in the northwest region when a balanced three-phase fault takes place at the midpoint of the Tana Beles to Bahir Dar 400 kV transmission line. The fault occurs at 6 s and is cleared at 6.25 s.

Table 3 presents the comparison of the system response for different variables with and without UPFC when 3ph-G fault occurred at the midpoint of the Tana Beles to Bahir Dar transmission line.

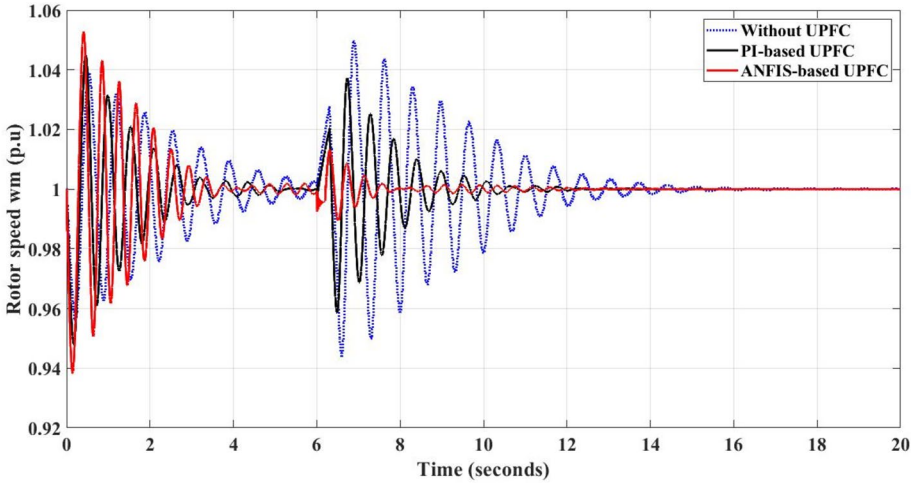

Fig. 14 Rotor speed response of Beles Unit-3 for 3ph-G fault occurred at the midpoint of the Tana Beles to Bahir Dar transmission line

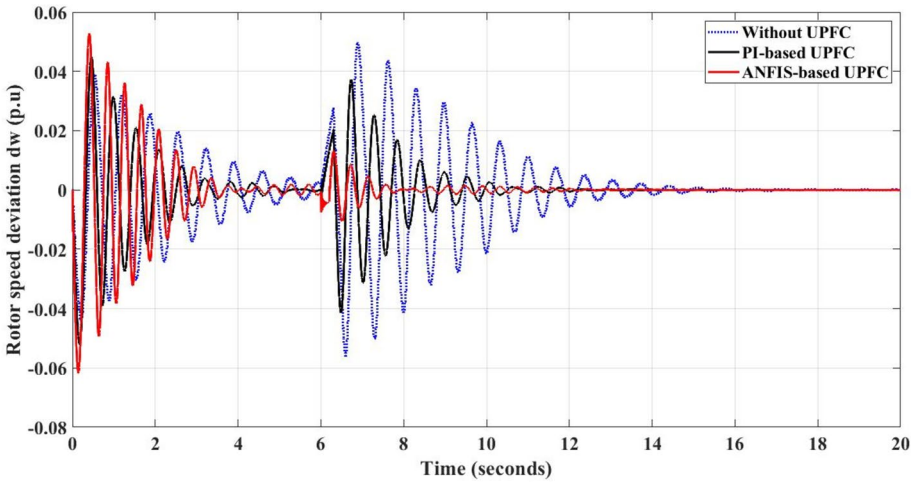

Fig. 15 Rotor speed deviation response of Beles Unit-3 for 3ph-G fault occurred at the midpoint of the Tana Beles to Bahir Dar transmission line

Sending-end and receiving-end active power for the NWR transmission line at peak load

The maximum real power transfer over a given transmission line can be increased by injecting a series voltage. As a result, voltage levels are increasing to allow large generating stations to transmit larger chunks of power over longer distances. Present-day high-voltage technology imposes limitations on increasing the voltage level for long overhead transmission lines.

Sending and receiving active power at peak load from Beles to Bahir Dar line

To increase the power transmitted in such cases, the only choice is to reduce the line reactance. This is accomplished by adding ANFIS-based UPFC. For NWR high-voltage transmission lines, this can be tested as shown in Fig. 17.

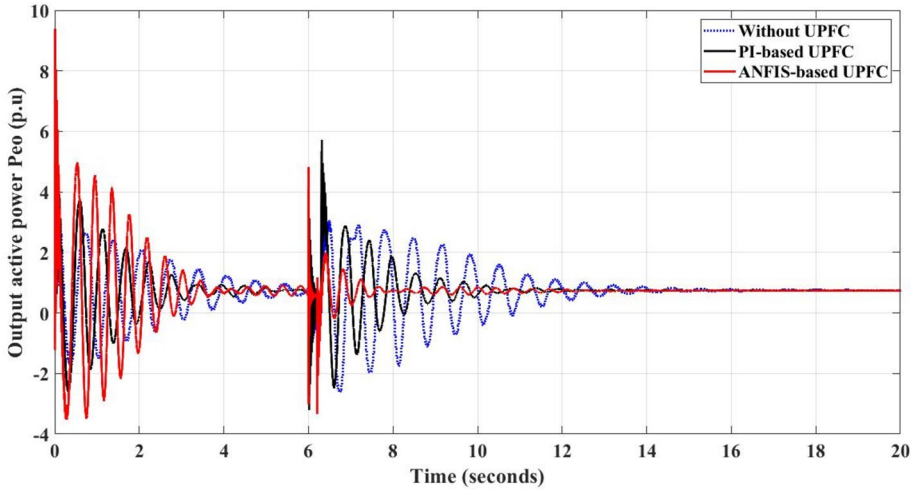

Fig. 16 Output active power response of Beles Unit-3 for 3ph-G fault occurred at the midpoint of the Tana Beles to Bahir Dar transmission line

Table 3 Comparison of the system response for different variables with and without UPFC when 3ph-G fault occurred at the midpoint of the Tana Beles to Bahir Dar transmission line

Variable type	Controller	Maximum peak value (Mp)	Percentage overshoot (%)	Settling time (sec)
Rotor angle deviation	Without UPFC	1.800	100.00	8.5
	PI-based UPFC	1.000	52.63	6.0
	ANFIS-based UPFC	0.300	12.50	2.5
Rotor speed	Without UPFC	0.050	5.00	9.8
	PI-based UPFC	0.039	3.90	6.3
	ANFIS-based UPFC	0.010	1.00	6.1
Rotor speed deviation	Without UPFC	0.050	5.00	9.8
	PI-based UPFC	0.039	3.90	6.3
	ANFIS-based UPFC	0.010	1.00	6.1
Output active power	Without UPFC	2.300	230.00	8.0
	PI-based UPFC	2.100	210.00	5.5
	ANFIS-based UPFC	0.100	10.00	4.5

The sending-end active power transferred at peak load from Tana Beles to Bahir Dar is 350 MW, while the receiving-end's active power without UPFC, with PI-based UPFC, and with ANFIS-based UPFC is 310, 330.5, and 338.6 MW, respectively. The receiving-end active power from Tana Beles to Bahir Dar transmission line without UPFC, with PI-based UPFC, with ANFIS-based UPFC, is shown in Figs. 18, 19, and 20.

The loss minimized after incorporating UPFC to the transmission line is presented in Table 4.

Voltage magnitude at all buses after incorporating UPFC to the system

Table 5 shows the magnitude of the bus voltage in p.u. at peak load after and before incorporating UPFC into the system. As expected, incorporating ANFIS-based UPFC

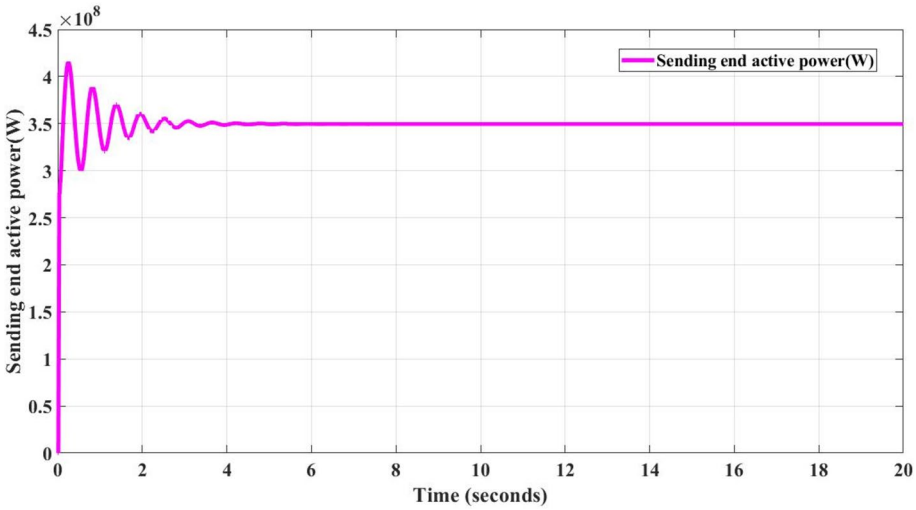

Fig. 17 Sending-end active power from Tana Beles to Bahir Dar transmission line

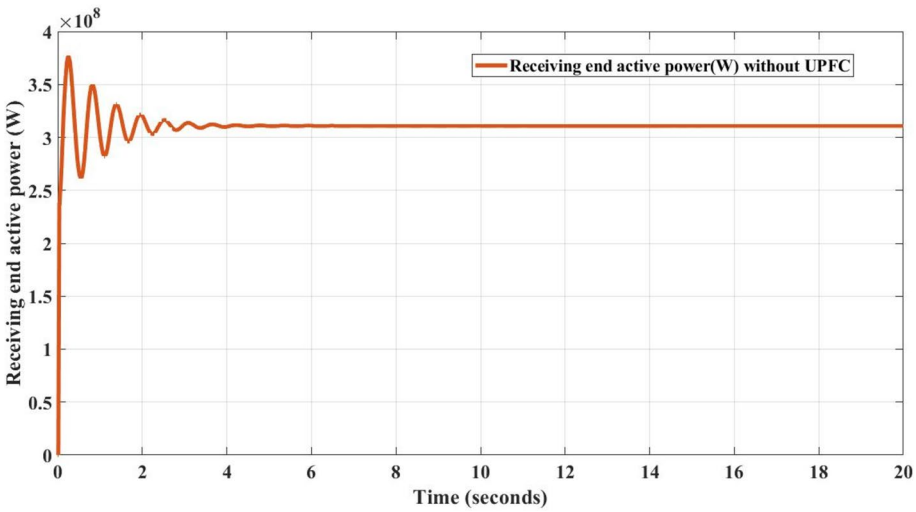

Fig. 18 Receiving-end active power from Tana Beles to Bahir Dar transmission line without UPFC

has maintained acceptable voltages at all buses in the system after being subjected to a disturbance and under normal operating conditions of the power system.

Waveforms of the northwest region 400 kV transmission line before and after UPFC series voltage injection

Waveforms of the northwest region 400 kV transmission line before and after UPFC series voltage injection is shown in the Fig. 21.

The peak voltage level before series injected voltage is 394 kV. The peak voltage levels after series injected voltage for both PI-based UPFC and ANFIS-based UPFC are 401 kV

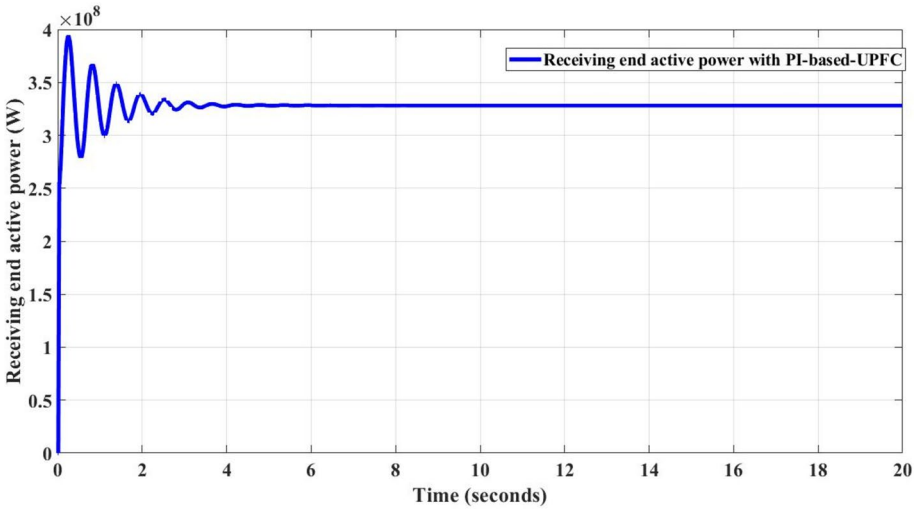

Fig. 19 Receiving-end active power from Tana Beles to Bahir Dar transmission line with PI-based UPFC

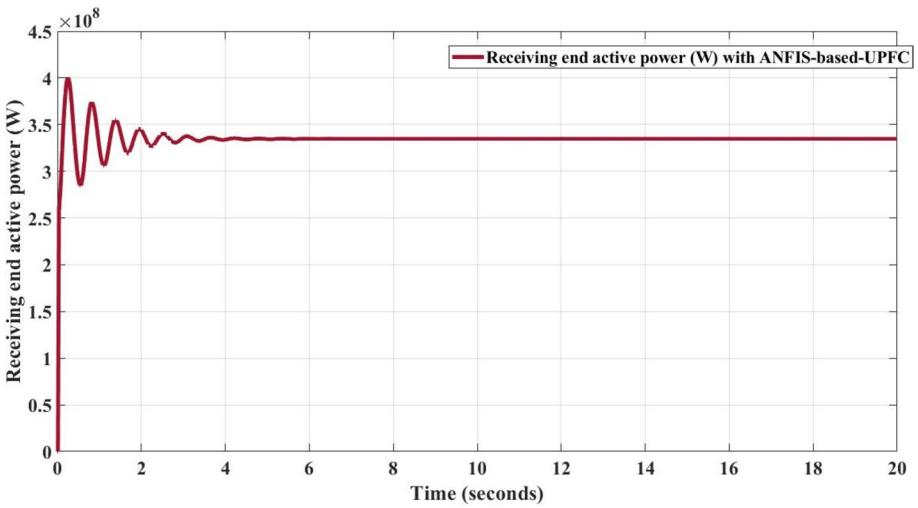

Fig. 20 Receiving-end active power from Tana Beles to Bahir Dar transmission line with ANFIS-based UPFC

Table 4 Loss minimized after incorporating UPFC to the transmission line

Controller	Receiving-end power (MW)	Power loss (MW)	Loss minimized (%)
Without	310	40	–
With PI-based UPFC	330.5	19.5	51.25
With ANFIS-based UPFC	338.6	11.4	71.50

and 418 kV, respectively. The result shows that the proposed ANFIS-based UPFC has better performance in improving line voltages than the PI-based UPFC. The percentages

Table 5 Voltage magnitude at all buses after incorporating UPFC to the system

Bus No	Bus location	Voltage magnitude (p.u) without UPFC	Voltage magnitude (p.u) with ANFIS-based UPFC
1	Tana Beles	1.0200	1.0200
2	Tis Abay II	1.0100	1.0100
3	Bahir Dar 400 kV	0.9365	0.9826
4	Bahir Dar 230 kV	0.9365	0.9651
5	Bahir Dar 132 kV	0.9532	0.9720
6	D/markos 400 kV	0.9532	1.0086
7	D/markos 230 kV	0.9432	1.0023
8	Motta 230 kV	0.9532	0.9845
9	Alamata 230 kV	0.9432	1.0047
10	Gonder I 230 kV	0.9570	0.9780
11	Gonder II 230 kV	0.9548	0.9782

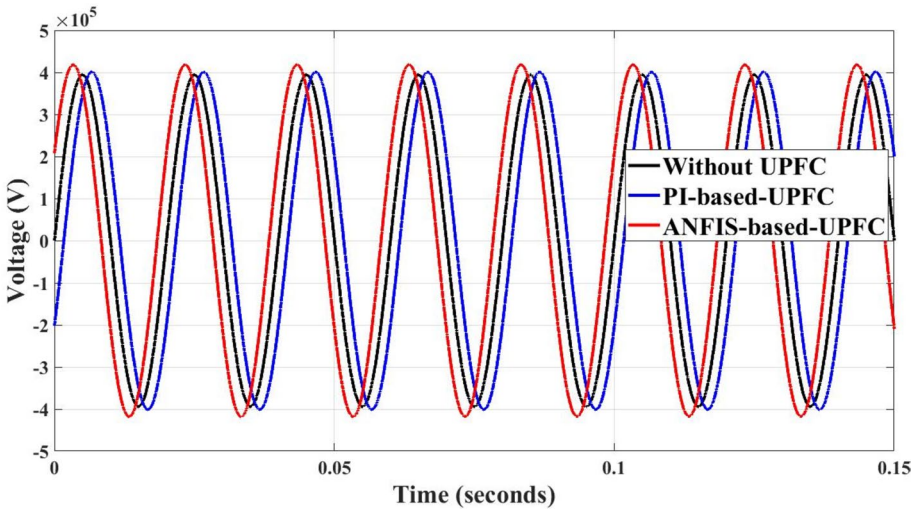

Fig. 21 The voltage waveforms of the NWR 400 kV transmission line before and after series injected voltage by UPFC

of voltage level improvement after series injection for both PI-based UPFC and ANFIS-based UPFC are 1.776% and 6.09%, respectively.

Conclusion

In this paper, we compared the transient stability of the ANFIS-based UPFC with PI-based UPFC in Ethiopia's 400 kV interconnected power system in the northwest region. This study employs a neuro-fuzzy inference system to effectively manage the power flow in high-voltage interconnected transmission power systems by utilizing the unified power flow controller (UPFC). To assess the effectiveness of the controller, three-phase-ground faults are induced in the system for analysis purposes. Also, to evaluate the performance of the power flow capability of transmission lines, peak load, average load, and minimum load have been applied to the system. This approach enables a higher utilization of the existing network, approaching its maximum thermal loading capacity, thereby eliminating the necessity to build new transmission lines.

The introduction of a three-phase ground fault at the midpoint of the Beles to Bahir Dar transmission line results in significant reductions in the settling time of various parameters when utilizing the ANFIS-based UPFC. Specifically, the rotor angle deviation, rotor speed, rotor speed deviation, and output active power of synchronous generators experience reductions of 70.58%, 37.75%, 37.75%, and 43.75%, respectively, compared to a system without UPFC. When operating at peak load on the Beles to Bahir Dar transmission line, the implementation of a PI-based UPFC and an ANFIS-based UPFC leads to substantial reductions in active power loss. Specifically, compared to a system without UPFC, the PI-based UPFC achieves a reduction of 51.25%, while the ANFIS-based UPFC achieves a greater reduction of 71.50%. Furthermore, under both normal operating conditions and when subjected to a disturbance, the ANFIS-based UPFC effectively ensures the preservation of acceptable voltages at all buses within the power system.

From the result, the neuro-fuzzy controller shows a lower settling time during the fault than a conventional PI-based UPFC controller. The simulation results clearly demonstrate that both the PI-based UPFC controller and the ANFIS-based UPFC greatly improve the transient stability and power transmission capability of the power system, based on the observations made.

Acknowledgements
I would like to express my deep and sincere gratitude to my advisor, Tefera Terefe Yetayew (Ph.D.) and Molla Addisu Mossie (Ph.D. Candidate), for allowing me to do the research and providing valuable guidance throughout this research.

Author contributions
Yechale Amogne Alemu provided the conceptualization, methodology, and formal analysis. Tefera Terefe Yetayew played a key role in designing the research framework, developing the methodology, and conducting the formal analysis of the data. Molla Addisu Mossie provided related work and edited the document.

Funding
This research did not receive any specific grant from funding agencies in the public, commercial, or not-for-profit sectors.

Availability of data and materials
Not applicable.

Declarations

Competing interests
The authors declare that there are no conflicts of interest.

Received: 6 December 2023 Accepted: 25 September 2024
Published online: 09 October 2024

References

1. Kundur P, Paserba J, Vite S (2003) Overview on definition and classification of power system stability. In: CIGRE/IEEE PES international symposium quality and security of electric power delivery systems
2. Zhu X, Jin M, Kong X et al (2018) Subsynchronous resonance and its mitigation for power system with unified power flow controller. J Mod Power Syst Clean Energy 6:181–189
3. Yuan Y, Li P, Kong X et al (2016) Harmonic influence analysis of unified power flow controller based on modular multilevel converter. J Mod Power Syst Clean Energy 4:10–18
4. Kumar RJ, Rammohan T (2020) Enhancement of transient stability in power system with multi-machine using facts device. In: IEEE international conference on advances and developments in electrical and electronics engineering (ICADEE), pp 1–7, Coimbatore
5. Kundur P (1994) Power system stability and control. McGraw-Hill, New York
6. Mihalic R, Zunko P, Povh D (1996) Improvement of transient stability using unified power flow controller. IEEE Trans Power Deliv 11(1):485–492
7. Balakrishnan FG, Sreedharan SK (2013) Transient stability improvement in power system using unified power flow controller (UPFC). In 2013 fourth international conference on computing, communications and networking technologies (ICCCNT), pp 1–6

8. Kumar Kavuturu KV, Sai Tejaswi KNV, Janamala V (2022) Performance and security enhancement using generalized optimal unified power flow controller under contingency conditions and renewable energy penetrations. J Electric Syst Inf Technol 18
9. Siddula S, Achyut TV, Vigneshwar K, Uday-Teja MV (2020) Improvement of power quality using fuzzy-based unified power flow controller. In: International conference on smart technologies in computing, electrical and electronics (ICSTCEE), pp 55–60
10. Jiang P, Fan Z, Feng S et al (2019) Mitigation of power system forced oscillations based on unified power flow controller. J Mod Power Syst Clean Energy 7:99–112
11. Ochoa-Giménez M, García-Cerrada A, Zamora-Macho JL (2017) Comprehensive control for unified power quality conditioners. J Mod Power Syst Clean Energy 5:609–619
12. Kumar R, Kumar M (2015) Improvement power system stability using unified power flow controller based on hybrid fuzzy logic-PID tuning in SMIB system. In 2015 international conference on green computing and internet of things (ICGCIoT), pp 815–819
13. Roy M, Kori AK (2021) FUZZY LOGIC based improvement of UPFC performance in power system. In: 2021 6th international conference on inventive computation technologies (ICICT), pp 245–250
14. Vetoshkin L, Votava J, Kyncl J, Müller Z (2019) Improvement of transient stability using STATCOM combined with optimization. In: 2019 20th international scientific conference on electric power engineering (EPE), pp 1–5, Prague, Czech Republic
15. Singh R, Kirar M (2016) Transient stability analysis and improvement in microgrid. In: 2016 international conference on electrical power and energy systems (ICEPES), pp 239–245, Bhopal, India
16. Luo Y, Yao J, Chen Z et al (2023) Transient synchronous stability analysis and enhancement control strategy of a PLL-based VSC system during asymmetric grid faults. Prot Control Mod Power Syst 8:35
17. Schauder CD et al (1998) Operation of the unified power flow controller (UPFC) under practical constraints. IEEE Trans Power Deliv 13(2):630–639
18. Morsli S, Tayeb A, Mouloud D, Abdelkader C (2012) A robust adaptive fuzzy control of a unified power flow controller. Turk J Elec Eng Comp Sci 20(1)
19. Aakula JL, Khanduri A, Sharma A (2020) Determining reactive power levels to improve bus voltages using PSO. In: 2020 IEEE 17th India council international conference (INDICON), New Delhi, India, pp 1–7
20. Latha S, Rani CK (2013) Transient stability improvement with unified power flow controller using fuzzy logic and ANFIS approach. Adv Mater Res 768(12):378–387
21. Singhal P, Agarwal SK, Kumar N (2014) Optimization of UPFC controller parameters using bacterial foraging technique for enhancing power system stability. Int J Adv Technol

Publisher's Note